ELSEVIER

Biochimica et Biophysica Acta 1192 (1994) 27–34

BBA Biochimica et Biophysica Acta

Dynamics of merocyanine 540 in model biomembranes: photoisomerization studies in small unilamellar vesicles

Yavuz Onganer, Edward L. Quitevis *

Department of Chemistry and Biochemistry, and Institute for Biotechnology, Texas Tech University, Lubbock, TX 79409, USA

(Received 15 October 1993)

Abstract

The fluorescence lifetime, τ_f, of merocyanine 540 (MC540) in small unilamellar vesicles was measured as a function of temperature and cholesterol content by using phase modulation fluorometry. These vesicles were formed by probe sonication of aqueous suspensions of egg phosphatidylcholine (PC) and cholesterol. The fluorescence lifetime of MC540 in these vesicles decreased with increasing temperature, but was independent of cholesterol. The decrease in τ_f with temperature is attributed to *trans-cis* photoisomerization. At low temperatures, the inverse of τ_f, or the fluorescence rate constant, k_f, approaches a constant value of 0.45 ± 0.02 ns^{-1}, which corresponds to the value of the radiative rate constant, k_r, of the dye. The photoisomerization rate constant, k_{iso}, was obtained by subtracting k_r from k_f. The temperature dependence of k_{iso} is well described by an Arrhenius equation, with an activation energy of 31.5 ± 0.9 kJ mol^{-1}. This Arrhenius behavior is rationalized in terms of the Smoluchowski limit for the Kramers theory for activated barrier crossing. The electronic spectra and k_{iso} for MC540 in these vesicles are consistent with the dye being located in the polar headgroup region of the lipid bilayer.

Key words: Merocyanine 540; Phosphatidylcholine; Cholesterol; Vesicle; Photoisomerization; Microviscosity

1. Introduction

Merocyanine 540 (MC540) is an anionic lipophilic polymethine dye (Fig. 1) that binds to biological and synthetic membranes [1–11]. The excited-state properties of MC540 are sensitive to electrical potential, and its fluorescence has been used to probe the transmembrane potential of many cell and organelle membranes [12–18]. It selectively stains and sensitizes the photoinactivation of leukemia cells, lymphoma cells, and enveloped pathogenic viruses [19–21]. The mechanism for the photodynamic activity of MC540, however, is not well understood [22–27]. By using spin label oximetry, Kalyanaraman et al. [22] observed the consumption of O_2 during photoexcitation of MC540 in unsaturated, but not in saturated liposomes. This observation suggested the possibility of peroxidation of unsaturated lipids, leading to membrane disruption. Inhibition by azide and enhancement by D_2O of the O_2 consumption point to singlet molecular oxygen, $O_2(^1\Delta_g)$, as the principle reactive intermediate in lipid peroxidation. Gaffney et al. [25] have recently demonstrated that MC540-mediated cell killing is O_2-dependent. Davila et al. [26,27] have proposed two alternate mechanisms for the highly efficient photodynamic activity of MC540. In their first mechanism, dye-based toxins, which arise from the oxidation of MC540 by $O_2(^1\Delta_g)$, are responsible for the chemotherapeutic activity of MC540. Davila et al. [27] argue that the high local viscosity in the membrane inhibits the diffusion of $O_2(^1\Delta_g)$. Therefore, oxidation reactions should be localized in the vicinity of the dye. Indeed, Gulliya et al. [21] have shown that irradiation of MC540 under aerobic conditions prior to incubation with leukemia cells results in cytoxic reagents. The second mechanism proposed by Davila et al. [27] is a thermalization mechanism which is based on the ability of the dye to undergo *trans–cis* photoisomerization about the central double bond (Fig. 1). The structural changes that occur upon photoisomerization could cause disruption of the membrane structure, allowing passage of ions through the membrane, and thereby killing the cell. During photoisomerization, the

* Corresponding author. Fax: +1 806 7421289.

SSDI 0005-2736(94)00026-L

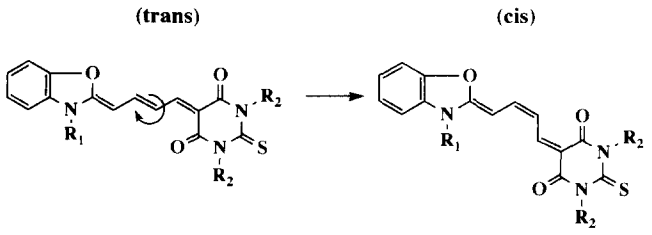

Fig. 1. Structure of merocyanine 540; $R_1 = (CH_2)_3SO_3^- Na^+$; $R_2 = (CH_2)_3CH_3$.

molecule undergoes S_1–S_0 internal conversion from the twisted state. The internal conversion process is accompanied by the dissipation of heat. Thus, the dye's cell killing ability could also arise from disruption of the membrane structure from local heating effects. In light of the lipid peroxidation experiments of Kalyanaraman et al. [22], cell thermalization probably does not contribute significantly to the photodynamic activity of MC540.

The photophysics and photochemistry of MC540 have been extensively investigated over the past several years [28–37]. Its photophysics are characterized by a normal state N and a photoisomer state P. Resonance Raman spectroscopy indicates that the N and P states are the *trans* and *cis* conformations of the molecule, respectively [36]. Because of the large barrier between the *trans* and *cis* forms in the ground electronic state, the dye mainly exists in the *trans* state [32,33]. In the first excited singlet state, the bond order of the central double bond of the polymethine chain is reduced, allowing the molecule to twist during its excited-state lifetime. In the twisted conformation, the molecule undergoes rapid internal conversion to the electronic ground state. From the twisted conformation, the molecule can relax either to the N-state or the P-state. Because the N-state is energetically lower than the P-state, the molecule eventually returns to the N-state. Recent studies in our laboratory have shown that the rate of photoisomerization of MC540 in polar solvents is inversely proportional to the solvent shear viscosity [37].

Experiments to date [30,32–34] show that photoisomerization is the dominant nonradiative relaxation pathway for the first excited singlet state of MC540 and that the rate of intersystem crossing is very slow. Until recently, it was thought that intersystem crossing occurred from the planar excited singlet state. Inhibiting photoisomerization should therefore increase the yield of the triplet states [28,29]. Since $O_2(^1\Delta_g)$ is formed by quenching of the triplet state of MC540 by O_2, the triplet yield sets the upper limit on the yield of $O_2(^1\Delta_g)$. However, Harriman [30] has now shown that the triplet state is more strongly coupled to the twisted excited singlet state than to the planar excited singlet state. Because of the extremely low rate of intersystem crossing from the planar excited singlet state, eliminating photoisomerization does not increase the triplet yield. Photoisomerization must therefore occur in order to form a significant yield of triplet states. Clearly, in order to elucidate the mechanism for the cell-killing ability of MC540, it is important to understand the effect of the membrane environment on photoisomerization.

Ideally, one would like to understand the photoisomerization dynamics in biological membranes. However, complications can arise because of the difficulty of separating effects due to the interactions of the dye with lipids and the dye with non-lipid constituents of a cell. In this paper we describe a study of the photoisomerization dynamics of MC540 in small unilamellar vesicles (SUVs), which serve as simple models for biomembrane systems.

Lelkes and Miller [4] studied the absorption spectra of MC540 in aqueous dipalmitoyllecithin dispersions and found that binding of MC540 to the vesicles is temperature-dependent. Below the gel-to-liquid-crystalline transition temperature, the absorption spectrum of the dye in these lipid dispersions is similar to that in pure water, with an absorption band around 500 nm. However, above the transition temperature, a new band appears at 562 nm, which is due to dye monomers interacting with lipids. These results suggest that the dye preferentially binds to lipid bilayers in the liquid-crystalline or fluid state rather than in the gel state. This conclusion was later confirmed by Williamson et al. [6], who observed that more dye binds to multilamellar vesicles and large (1000 Å diameter) unilamellar vesicles that are in the fluid-phase state than to comparable vesicles that are in the gel-phase state. Furthermore, small (200–300 Å diameter) unilamellar gel-phase vesicles, which because of their small radius of curvature behave like liquid-crystalline phase bilayers, bind more dye than large unilamellar gel-phase vesicles. Clearly, the temperature-dependent binding properties of MC540 to lipid bilayers complicate the analysis of the photoisomerization dynamics of the dye, if one wishes to measure the temperature dependence of the photoisomerization rate. In order to avoid these complications, our photoisomerization studies were carried out by using egg-phosphatidylcholine (PC)/cholesterol SUVs. Cogan et al. [38] have shown that egg-PC/cholesterol vesicles are in the liquid-crystalline phase over a wide range of temperatures.

This photoisomerization study of MC540 in egg-PC/cholesterol vesicles was also motivated by the fact that cholesterol alters the membrane microviscosity. We had thought that since the photoisomerization rate constant depends inversely on the viscosity, the photodynamic activity of MC540 should be higher in membrane systems containing less cholesterol. Indeed,

Shinitzky and Inbar [40] analyzed the fluorescence depolarization of 1,6-diphenyl-1,3,5-hexatriene (DPH) in intact cells and in liposomes prepared from lipid extracts of these cells. They showed that the microviscosity in the surface membrane lipid layer was greater for normal lymphocytes than for lymphoma cells. Furthermore, the relative amount of cholesterol in a lymphoma cell is about half that of a normal lymphocyte. This would be consistent with the tendency of malignant cells to bind more dye than normal cells due to the increase in the membrane fluidity. However, we will show in this paper that the amount of cholesterol appears to have no effect on the photoisomerization rate constant of MC540 in egg-PC/cholesterol SUVs.

2. Materials and methods

2.1. Chemicals

Egg PC (Avanti Polar) and cholesterol (Sigma) were used without further purification. Cholesterol was stored as a solid at −20°C. Egg PC was stored as a 100 mg/ml solution in chloroform at −20°C. MC540 (Molecular Probes or Sigma) and rhodamine 101 (Rh101) (Exciton, laser grade) showed single spots on a thin-layer chromatography plate and were used without further purification. MC540 was stored in the dark as a concentrated stock solution (1 mM) in an ethanol/carbon tetrachloride mixture (1 : 1, v/v).

2.2. Vesicle preparation

A 50-μl aliquot of the egg-PC stock solution was spread on the walls of a tube and first dried under nitrogen and then under vacuum for 2 h to remove the solvent. The dried lipid sample was hydrated with 2 ml of physiological saline solution buffered at pH 7.4 (NBS primary buffer 0.0087 M KH_2PO_4, 0.034 M Na_2HPO_4, 0.1 M KCl). SUVs were formed by ultrasonic dispersal of the hydrated lipid sample at room temperature (≈ 21°C) under nitrogen. The microtip of a Sonics and Materials Model VC 300 Ultrasonic Processor was used. The sonicator was set at 250 W for 2 h at a duty cycle of 50%. The fact that the resulting solution was clear indicated that all of the lipid was dispersed in solution. The sample was centrifuged on a IEC Micro-MB Model 3615 microcentrifuge at 14000 rpm for 30 min to remove the small metal pieces that break off the microtip during sonication. The lipid dispersion was then diluted to obtain the desired lipid concentration. To prepare the cholesterol-containing vesicles, cholesterol was added to egg-PC in chloroform prior to drying. The resulting mixture was then processed as described above. The vesicles were labelled with dye by evaporating 12 μl of the MC540 stock solution and then redissolving with 4 ml of the lipid dispersion. The final dye concentration was ≈ 3 μM, with the lipid-to-dye mole ratio being 300 : 1.

2.3. Steady-state spectroscopy and fluorescence lifetime measurements

Excitation (uncorrected) and fluorescence (corrected) spectra were recorded on an SLM Aminco 4800C fluorometer. Fluorescence lifetimes were measured by phase modulation fluorometry with this instrument. The samples were contained in a 1-cm cuvette in the fluorometer. The temperature of the sample was controlled to ±1°C by flowing water through the cell holder in the fluorometer with a temperature-controlled water circulator (Neslab RTE-4). The temperature in the cuvette was measured with a thermometer. In the fluorescence lifetime measurements, the excitation and emission monochromators were set, respectively, at 520 and 575 nm. A polarizer set to 54.7° ('magic angle') with respect to the polarization of the excitation light was placed between the emission monochromator and the sample to remove molecular reorientation effects. Rh101 in ethanol was used as the reference for the fluorescence lifetime measurements. Our measured value of τ_f for Rh101 in ethanol at 25°C compared well with the literature value of 5.3 ns [41] when we used other dyes with known fluorescence lifetimes as references. The value of τ_f for Rh101 obtained by using Rhodamine 6G in ethanol (τ_f = 3.85 ns) [42], rhodamine B (RhB) in acidic ethanol (τ_f = 2.3 ns) [43–46], and RhB in basic ethanol (τ_f = 2.7 ns) [43,46] as references, were 5.30, 5.26, and 5.31 ns, respectively.

3. Results

3.1. Steady-state spectra

Fig. 2 illustrates the excitation and fluorescence spectra of 3 μM MC540 in two lipid dispersions and in pure water. The spectra of the dye in these lipid dispersions are red-shifted from the spectrum of the dye in water. The peak of the excitation spectrum occurs at λ_e = 567, 567, 568, and 569 nm for MC540 in the lipid dispersions containing 0, 10, 20, and 30 mol% cholesterol, respectively. Correspondingly, the peak of the fluorescence spectrum occurs at λ_{fl} = 591, 593, 594, and 594 nm for MC540 in the lipid dispersions containing 0, 10, 20, and 30 mol% cholesterol, respectively. The uncertainty in these wavelength maxima is ±1 nm. These spectra indicate a slight red shift as the cholestrol content is increased. The spectral properties of MC540 in these vesicles are similar to those of MC540 in the higher alcohols (i.e., λ_e = 567 nm, λ_{fl} = 592 nm

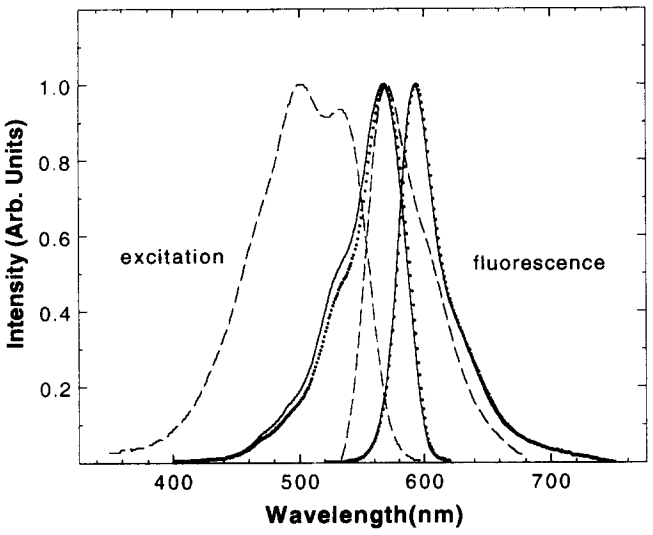

Fig. 2. Normalized excitation (uncorrected) and fluorescence (corrected) spectra of 3 μM MC540 in pure water (dashed curves) egg-PC (dotted curves) and egg-PC/cholesterol (30 mol%) (solid curves) SUVs.

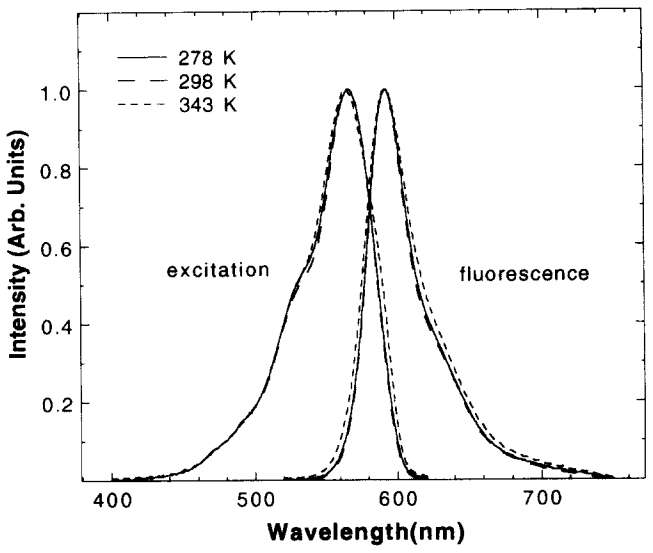

Fig. 3. Temperature dependence of the normalized excitation (uncorrected) and fluorescence (corrected) spectra of MC540 in egg-PC/0 mol% cholesterol SUVs.

in 1-octanol [37]). Changing the temperature had very little effect on the shape or the position of the spectra, as illustrated in Fig. 3.

3.2. Fluorescence lifetimes

As can be seen in Table 1, τ_f exhibits a strong dependence on temperature. It remains fairly constant for temperatures between 278 and 293 K, but then rapidly decreases for temperatures greater than 293 K. In contrast, within experimental error, cholesterol does not greatly affect the fluorescence lifetime of MC540 in these lipid dispersions.

3.3. Photoisomerization rate

The inverse of the fluorescence lifetime, k_f, (the fluorescence rate) is related to the radiative rate constant, k_r, and the nonradiative rate constant, k_{nr}, by the equation

$$k_f = 1/\tau_f = k_r + k_{nr} \quad (1)$$

where

$$k_{nr} = k_{ic} + k_{isc} + k_{iso} \quad (2)$$

In this equation, k_{ic}, k_{isc}, and k_{iso} are the rate constants for internal conversion, intersystem crossing, and photoisomerization from the excited N-state, respectively. Because the triplet quantum yield for MC540 is typically less than 0.05 in the temperature range of our measurements [30,32,33], k_{isc} can be neglected relative to $k_{ic} + k_{iso}$. Hoebeke et al. [34] measured the fluorescence quantum yield, Φ_f, and the photoisomerization quantum yield, Φ_{iso}, for MC540 in glycerol/ethanol mixtures. By varying the relative amounts of glycerol and ethanol, they were able to vary the viscosity of the

Table 1
Fluorescence lifetime of merocyanine 540 in egg phosphatidylcholine/cholesterol vesicles as a function of temperature

Temperature (K)	τ_f (ns) [a,b]			
	0 mol% cholesterol	10 mol% cholesterol	20 mol% cholesterol	30 mol% cholesterol
278	2.37 ± 0.03	2.18 ± 0.02	2.15 ± 0.02	2.10 ± 0.02
283	2.33 ± 0.03	2.15 ± 0.02	2.16 ± 0.02	2.11 ± 0.02
288	2.26 ± 0.04	2.08 ± 0.02	2.07 ± 0.02	2.07 ± 0.03
293	2.19 ± 0.02	2.05 ± 0.04	2.01 ± 0.03	1.97 ± 0.03
298	1.93 ± 0.03	1.79 ± 0.03	1.86 ± 0.02	1.87 ± 0.03
308	1.69 ± 0.02	1.64 ± 0.03	1.63 ± 0.03	1.65 ± 0.04
323	1.42 ± 0.02	1.31 ± 0.04	1.32 ± 0.03	1.43 ± 0.03
333	1.17 ± 0.03	1.20 ± 0.02	1.17 ± 0.04	1.28 ± 0.04
343	1.09 ± 0.03	1.15 ± 0.03	1.07 ± 0.02	1.21 ± 0.03

[a] Each value of τ_f in the table is the average of at least three measurements (± S.D.).
[b] Column headings correspond to the cholesterol content in the vesicles.

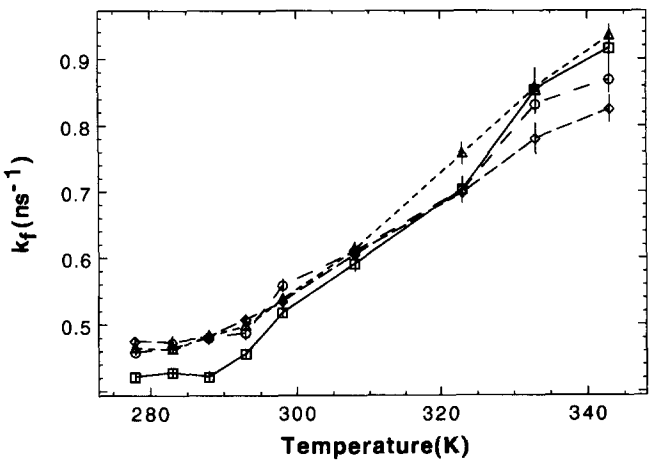

Fig. 4. Plot of fluorescence rate constant, k_f, versus temperature for merocyanine 540 in egg-PC/cholesterol SUVs with the following amounts of cholesterol: 0 mol% (□); 10 mol% (○); 20 mol% (△); 30 mol% (◇). Values of k_f obtained from the inverse of the fluorescence lifetime, τ_f (Table 1).

mixtures. They found that as the viscosity of the mixtures increased, Φ_f increased while Φ_{iso} decreased, with $\Phi_f + \Phi_{iso} \approx 1$ for all values of the viscosity. Aramendia et al. [32,33] showed further that the photoisomer of MC540 arises directly from the first excited singlet state. These results indicate that k_{ic} can be neglected relative to k_{iso}. Therefore, for MC540, photoisomerization is the dominant nonradiative process, and the nonradiative rate constant in Eq. (1) can be essentially set equal to k_{iso}:

$$k_f \approx k_r + k_{iso} \quad (3)$$

Fig. 4 illustrates the variation of k_f with temperature for the four vesicle systems. Between 278 and 288 K, the fluorescence rate constant for MC540 in these lipid bilayers approaches a constant value, the average of which is 0.45 ± 0.02 ns^{-1}. Above 288 K, the fluorescence rate constant starts to increase, with the value of k_f at 343 K roughly double the value of k_f below 288 K. This dependence on temperature is consistent with Eq. (3). According to this equation, the fluorescence rate constant should decrease as the temperature is decreased, due to a decrease in the photoisomerization rate constant. However, because the radiative rate constant is independent of temperature, the fluorescence rate constant will approach a constant value corresponding to the value of k_r. The low-temperature limiting value of k_f agrees with the average literature value of k_r of 0.45 ± 0.04 ns^{-1} [26,27,33,37].

The photoisomerization rate constant, k_{iso}, can be obtained by subtracting the low-temperature limiting value of k_f, which we have shown to be essentially equal to the value of k_r, from the values of k_f at the various temperatures. The resulting values of k_{iso} are listed in Table 2 for MC540 in each of the vesicle systems, along with the values of k_r. Upon examining the values of k_{iso}, we conclude that the photoisomerization dynamics of MC540 in these lipid dispersions is largely independent of the cholesterol content and that the temperature dependence of k_{iso} is essentially the same for all of these systems. This allows us to calculate an average value for k_{iso} (column 6, Table 2) in these lipid dispersions. These values are used to construct an Arrhenius plot for k_{iso}. A plot of ln k_{iso} versus $1/T$ (Fig. 5) is linear (correlation ≥ 0.98) over the temperature range of 298 to 343 K. The linearity of this Arrhenius plots is consistent with k_{iso} being given by an Arrhenius equation

$$k_{iso} = A_{iso} \exp(-E_a/RT) \quad (5)$$

Linear regression of ln k_{nr} versus $1/T$ leads to a value of 31.5 ± 0.9 kJ mol^{-1} for the activation energy, E_a. The calculation of the error in the value of E_a has been described previously [37]. It is interesting to note

Table 2
Photoisomerization rate constant of merocyanine 540 in phosphatidylcholine/cholesterol vesicles as a function of temperature

Temperature (K)	k_{iso} (ns^{-1})				
	0 mol% cholesterol [a,f]	10 mol% cholesterol [b,f]	20 mol% cholesterol [c,f]	30 mol% cholesterol [d,f]	Average value [e,g]
298	0.10 ± 0.01	0.10 ± 0.01	0.075 ± 0.007	0.061 ± 0.007	0.084 ± 0.019
308	0.17 ± 0.01	0.15 ± 0.02	0.15 ± 0.01	0.13 ± 0.02	0.15 ± 0.02
323	0.28 ± 0.02	0.30 ± 0.02	0.30 ± 0.02	0.23 ± 0.02	0.28 ± 0.03
333	0.43 ± 0.02	0.37 ± 0.01	0.40 ± 0.03	0.31 ± 0.03	0.38 ± 0.05
343	0.50 ± 0.03	0.41 ± 0.02	0.47 ± 0.02	0.35 ± 0.02	0.43 ± 0.07

Values of k_{iso} obtained from $k_f - k_r$, where k_r is the low temperature limit of k_f (see Fig. 4).
[a] $k_r = 0.422 \pm 0.005$ ns^{-1};
[b] $k_r = 0.459 \pm 0.004$ ns^{-1};
[c] $k_r = 0.463 \pm 0.004$ ns^{-1};
[d] $k_r = 0.474 \pm 0.009$ ns^{-1};
[e] Average value of k_{iso} over all four vesicle systems.
[f] Errors obtained by propagating the errors in k_f and k_r;
[g] Error = standard deviation (S.D.).

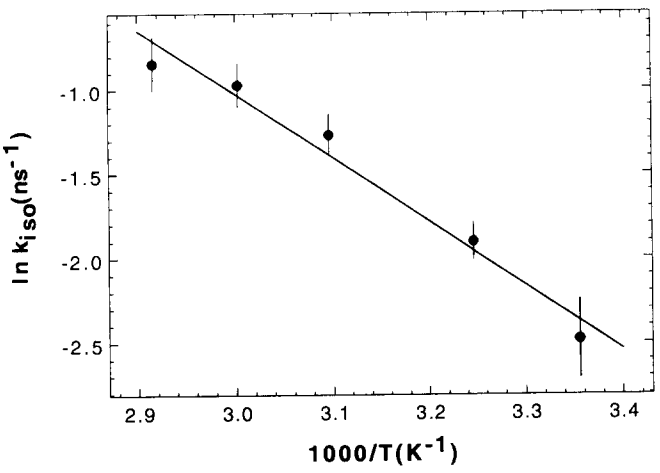

Fig. 5. Arrhenius plot of the average of the photoisomerization rate constant, k_{iso}, for merocyanine 540 in egg-PC/cholesterol SUVs. See Table 2 for values of k_{iso}. Line is a linear least-squares fit to the data. Intercept = 10.358, slope = −3.794, correlation = −0.986.

that the value of E_a for MC540 in vesicles is ≈ 6 kJ mol^{-1} higher than the value of E_a for MC540 in 1-octanol (25 ± 3 kJ mol^{-1}) [37].

4. Discussion

4.1. Steady spectra

MC540 is a positive solvatochromic dye which exhibits a bathochromic shift with decreasing solvent polarity. The values of λ_e for MC540 in solvents correlate strongly with the dielectric constant ϵ, with λ_e decreasing with ϵ [4]. Therefore, the dye spectrum provides a way of establishing the nature of the microenvironment of the dye within the lipid bilayer. The values of λ_e and λ_{fl} for MC540 in these lipid dispersions indicate that the microenvironment around MC540 in a bilayer can be characterized by a polarity similar to that of 1-octanol or higher alcohols. Lelkes and Miller [4] combined solvent polarity studies with the spectral appearance of MC540 bound to phospholipids to show that the dye is in the vicinity of the polar region of the lipid bilayer. Based on the dye's molecule structure, they hypothesized that the dye is anchored to the hydrocarbon chain region through the two tetramethylenic tails, with the rest of the molecule lying near the ester bonds. The benzoxazole end, which is functionalized with an anionic sulfonate group, points towards the polar outer surface of the headgroup region. Such an orientation gives rise to a microenvironment having a polarity similar to that of the higher alcohols. The absence of any significant change in the shape of the electronic spectra of MC540 in these vesicles with temperature is consistent with our initial conjecture that because egg-PC/cholesterol SUVs are in the liquid crystalline state, the dye primarily exists as vesicle-bound dye in these systems.

4.2. Photoisomerization rate

Onganer et al. [37] showed that the photoisomerization rate constant of MC540 in polar solvents can be described by the high friction limit of Kramers theory for activated barrier crossing. In the Kramers theory, the reaction is modeled by the motion of a particle in a one-dimensional potential, with the motion modified by frictional drag and a random fluctuating force [47]. In this theory the rate constant is given by

$$k_{iso} = F(\zeta)\ \exp(-E_0/RT) \tag{6}$$

where E_0 is the intrinsic barrier height, R is the gas constant, and T is the absolute temperature. The prefactor, $F(\zeta)$, is a dynamical factor that depends on the friction, ζ, that is felt by the isomerizing groups. In the Smoluchowski limit (the high friction limit), $F(\zeta)$ becomes inversely proportional to friction

$$F(\zeta) = \omega_r \omega_b I_r / 2\pi\zeta \tag{7}$$

where ω_r is the reactant well frequency, ω_b is the barrier frequency, and I_r is the reduced moment of inertia for the isomerizing moieties. The friction is not an experimentally observable quantity. However, for MC540 in polar solvents, a hydrodynamic model can be used for the friction. In the hydrodynamic model, the friction is proportional to the solvent shear viscosity, η, i.e., $\zeta = f\eta$. The hydrodynamic form of the Smoluchowski limit of the rate constant reduces to

$$k_{iso} = (B/\eta)\ \exp(-E_0/RT) \tag{8}$$

where B is given by $\omega_r \omega_b\ I_r/2\pi\zeta$. Eq. (8) can be converted into a more useful form by replacing η by the empirical equation

$$\eta = \eta_0\ \exp(E_\eta/RT) \tag{9}$$

where E_η is the viscosity activation energy. Combining Eqs. (8) and (9) yields the following expression for the rate constant

$$k_{iso} = (B/\eta_0)\ \exp\left[-(E_0 + E_\eta)/RT\right] \tag{10}$$

Eq. (10) is an Arrhenius-type equation with the overall activation energy E_a equal to the sum $E_0 + E_\eta$. The excellent agreement with Arrhenius behavior that is displayed in Fig. 5 strongly suggests that the Smoluchowski limit of Kramers theory adequately describes the photoisomerization dynamics of this dye in bilayer membranes.

The applicability of the Smoluchowski limit to MC540 in these systems, permits us to consider an alternate way of determining the relative microviscosities in lipid bilayers. In previous studies [38,48], the fluorescence depolarization associated with hydropho-

bic fluorescent probes was used to monitor the fluidity in the hydrophobic region of of phospholipid bilayers. By assuming that the probe molecules undergo isotropic rotational diffusion in the hydrophobic region, the steady-state fluorescence anisotropy can be related to an apparent microviscosity by means of a modified version of the Perrin equation. Although such an interpretation may be valid for small fluorescent probes, time-resolved fluorescence depolarization studies [49–51] have shown that rod-like probes, such as DPH, undergo hindered or restricted rotational diffusion in lipid bilayer membranes. In lipid bilayer membranes, the time-resolved fluorescence anisotropy, $r(t)$, is a maximum at the point of excitation and decays to a constant value, r_∞, after a period of time. The decay time, ϕ, is proportional to the microviscosity of probe's local membrane environment. The constant value of the anisotropy is related to the order parameter of the membrane. MC540 is considered to be a rod-like molecule from the point of view of its reorientational dynamics in liquids [52]. Thus, it is not surprising that variable frequency cross-correlation phase fluorometry indicates that the reorientational dynamics of MC540 in lipid bilayers are best described in terms of restricted rotational diffusion (Onganer, Y., Chen, S.-Y., Cheng, K.H. and Quitevis, E.L., unpublished data). For rod-like molecules, the steady-state fluorescence anisotropy is comprised of a dynamic component and a static or structural component. Therefore, microviscosities obtained from steady-state fluorescence anisotropy measurements of MC540 in vesicles would have dubious value, because of the anisotropic nature of the reorientational dynamics for this dye in lipid bilayers.

We attribute the increase in the rate of photoisomerization for MC540 with increasing temperature in a given lipid bilayer to a decrease in the microviscosity of the probe's local environment with increasing temperature. When comparing the photoisomerization rate constant in different membrane systems, one must be careful about making statements concerning the relative microviscosities in these systems, because the rate also depends on the polarity of the microenviroment. This polarity dependence is manifested in solvent-induced variations in the intrinsic barrier height, E_0, and in the prefactor B. Because of the sensitivity of the electronic spectra of MC540 to the polarity of the dye's environment, systems for which the electronic spectra of the dye are similar should display the same polarity effects on the photoisomerization dynamics. Since the spectra of MC540 in these vesicles are similar to those of MC540 in the higher alcohols, the polarity effects in these vesicles must be very similar to that in the higher alcohols. Onganer et al. [37] showed that to a large extent, the polarity in these higher alcohols plays less of a role in determining the photoisomerization dynamics than does the viscosity of the solvent. Consequently, the overall activation energy is higher in lipid bilayers than in 1-octanol, because the microviscosity activation energy is slightly higher in lipid bilayers than in 1-octanol.

The similarity of the steady-state spectra of MC540 in the four vesicle systems with differing amounts of cholesterol implies that the effect of polarity on k_{iso} must be the same in these lipid bilayer systems. The absence of a dependence of k_{iso} on the cholesterol content in these SUVs must be primarily due to the fact that the dye is located at the surface of the bilayer and not in the hydrocarbon region of the bilayer. By measuring the rotational diffusion of small nonpolar fluorescent probes through steady-state fluorescence depolarization, Cogan et al. [38] found that increasing the cholesterol content increases the microviscosity in dipalmitoyllecithin-cholesterol lipid dispersions. These apolar probes tend to be located in the hydrocarbon core of the bilayer. The microviscosity in this region is not necessarily going to have the same value in the polar region, which is the binding site for MC540 in lipid bilayers. Cholesterol inserts deeply into the bilayer with its long axis oriented normal to the bilayer plane [53]. In this orientation, the β-OH group on the sterol moiety points towards the polar headgroup region, while the hydrocarbon tail points towards the apolar core of the bilayer. X-ray and neutron scattering [54] show the β-OH group is near the ester carbonyl of the lipid. However, no hydrogen bond is formed with these carbonyls, as indicated by Raman spectroscopy [55]. The increase in the microviscosity in the hydrocarbon core of the bilayer occurs because the rigid sterol moiety prevents the adjacent acyl chains from packing. Thus, in the fluid state of the lipid bilayer, the sterol conformationally constrains the chains, whereas in the gel state the sterol prevents the packing of the all-*trans* chain configuration. In contrast, cholesterol-lipid interactions have little effect on the conformation of the headgroups [53].

In conclusion, this study has shown that the photoisomerization of MC540 in egg-PC/cholesterol SUVs is consistent with the Smoluchowski or high friction limit of the Kramers theory. The dependence of k_{iso} with temperature is due partly to the decrease in the microviscosity of the dye's local membrane environment with increasing temperature. The spectra indicate that the polarity of the dye's membrane microenvironment is comparable to that in the higher alcohols. The lack of an effect of cholesterol on k_{iso} is attributed to the dye being primarily located in the polar headgroup region of the lipid bilayer. Clearly, time-resolved fluorescence depolarization measurements of MC540 in these membranes will help to confirm these results, by allowing us to measure rotational diffusion constants and order parameters. Based on the recent photophysi-

cal results of Harriman [30], it clear that photoisomerization must occur in order to form the triplet state and consequently singlet oxygen. Therefore, being located in the polar headgroup region, and not buried in the highly viscous region of hydrocarbon region of the bilayer, should facilitate the formation of singlet oxygen. Although our results indicate that the cholesterol content does not affect the photophysics of the dye in a lipid bilayer, the cholesterol content may still play an indirect role in the dye's photodynamic efficacy by affecting the binding of the dye to a cell. Cholesterol increases order in the bilayer. Based on the hypothesis that MC540 binds preferentially to disordered domains in the lipid bilayer, bilayers containing less cholesterol should bind more dye. This would partly explain why malignant cells bind more dye than normal cells. As previously stated by Sieber [20], the ability of a cell to bind more dye may be the most important factor in determining a cell's photosensitivity.

Acknowledgements

This work was supported by the National Institutes of Health through Grant R15-GM42192-01 and by the Robert A. Welch Foundation through Grant D-1019 to E.L.Q.

References

[1] Pohl, G.W. (1976) Z. Naturforsch. 31C, 575–588.
[2] Easton, T.G., Valinsky, J.E. and Reich, E. (1978) Cell 13, 475–486.
[3] Valinsky, J.E., Easton, T.G. and Reich, E. (1978) Cell 13, 487–499.
[4] Lelkes, P.I. and Miller, I.R. (1980) J. Membr. Biol. 52, 1–15.
[5] Williamson, P., Massey, W. A, Phelps, B.M. and Schlegel, R.A. (1981) Mol. Cell. Biol. 1, 128–135.
[6] Williamson, P., Mattocks, K. and Schlegel, R.A. (1983) Biochim. Biophys. Acta 732, 387–393.
[7] Verkman, A.S. and Frosch, M.P. (1985) Biochemistry 24, 7117–7122.
[8] Verkman, A.S. (1987) Biochemistry 26, 4050–4056.
[9] Guarcello, V., Stern, A. and Rizza, V. (1987) Biochim. Biophys. Acta 917, 318–323.
[10] Dodin, G., Aubard, J. and Falque, J. (1987) J. Phys. Chem. 91, 1166–1172.
[11] Dodin, G. and Dupont, J. (1987) J. Phys. Chem. 91, 6322–6326.
[12] Waggoner, A. (1976) J. Membr. Biol. 27, 317–334.
[13] Waggoner, A. (1979) Annu. Rev. Biophys. Bioeng. 8, 47–68.
[14] Waggoner, A.S. and Grinvald, A. (1977) Ann. N.Y. Acad. Sci. 303, 217–241.
[15] Waggoner, A.S. (1979) Methods Enzymol. 55, 689–695.
[16] Salama, G. and Morad, M. (1976) Science 191, 485–487.
[17] Tasaki, I. and Warashina, A. (1976) Photochem. Photobiol. 24, 191–207.
[18] Dragsten, P.R. and Webb, W.W. (1978) Biochemistry 17, 5228–5240.
[19] Sieber, F., Spivak, J.L. and Sutcliffe, A.M. (1984) Proc. Natl. Acad. Sci. USA 81, 7584–7587.
[20] Sieber, F. (1987) Photochem. Photobiol. 46, 1035–1042.
[21] Gulliya, K.S., Pervaiz, S., Dowben, R.M. and Mathews, J.L. (1990) Photochem. Photobiol. 52, 831–839.
[22] Kalyanaraman, B., Feix, J.B., Sieber, F., Thomas, J.P. and Girotti, A.W. (1987) Proc. Natl. Acad. Sci. USA 84, 2999–3003.
[23] Feix, J.B. and Kalyanaraman, B. (1991) Photochem. Photobiol. 53, 39–45.
[24] Feix, J.B. and Kalyanaraman, B. (1991) Arch. Biochem. Biophys. 1, 43–51.
[25] Gaffney, D.K., O'Brien, J. and Sieber, F. (1991) Photochem. Photobiol. 53, 85–92.
[26] Davila, J., Gulliya, K.S. and Harriman, A. (1989) J. Chem. Soc., Chem. Commun., 1215–1216.
[27] Davilia, J., Harriman, A. and Gulliya, K.S. (1991) Photochem. Photobiol. 53, 1–11.
[28] Krieg, M. (1992) Biochim. Biophys. Acta 1105, 333–335.
[29] Hoebeke, M., Seret, A., Piette, J. and Van de Vorst, A. (1988) J. Photochem. Photobiol. B. Biol. 1, 437–446.
[30] Harriman, A. (1992) J. Photochem. Photobiol. A. Chem. 65, 79–93.
[31] Dixit, N.S. and Mackay, R.A. (1983) J. Am. Chem. Soc. 105, 2928–2929.
[32] Aramendia, P.F., Kreig, M., Nitsch, C., Bittersmann, E. and Braslavsky, S.E. (1988) Photochem. Photobiol. 48, 187–194.
[33] Aramendia, P.F., Duchowicz, R., Scaffardi, L. and Tocho, J.O. (1990) J. Phys. Chem. 94, 1389–1392.
[34] Hoebeke, M., Piette, J. and Van de Vorst, A. (1990) J. Photochem. Photobiol. B. Biol. 4, 273–282.
[35] Hoebeke, M., Seret, A., Piette, J. and Van de Vorst, A. (1991) J. Photochem. Photobiol. B. Biol. 9, 281–294.
[36] Harriman, A., Shoute, L.C.T. and Neta, P. (1991) J. Phys. Chem. 95, 2415–2420.
[37] Onganer, Y., Yin, M., Bessire, D.R. and Quitevis, E.L. (1993) J. Phys. Chem. 97, 2344–2354.
[38] Cogan, U., Shinitzky, M., Weber, G. and Nishida, T. (1973) Biochemistry 12, 521–528.
[39] Humphries, G.M.K. and Lovejoy, J.P. (1983) Biochem. Biophys. Res. Commun. 111, 768–774.
[40] Shinitzky, M. and Inbar, M. (1974) J. Mol. Biol. 85, 603–615.
[41] Karsten, T. and Kobs, K. (1980) J. Phys. Chem. 84, 1871–1872.
[42] López Arbeloa, F., López Arbeloa, T., Lage, E. Gil, López Arbeloa, I. and De Schryver, F.C. (1991) J. Photochem. Photobiol. A. Chem. 56, 313–321.
[43] López Arbeloa, T., Estévez, M.J., López Arbeloa, F., Aguirresacona, I. Urretxa and López Arbeloa, I. (1991) J. Lumin. 48 and 49, 400–404.
[44] Drake, J.M., Morse, R.I., Steppel, R.N. and Young, D. (1975) Chem. Phys. Lett. 35, 181–188.
[45] Casey, K.G. and Quitevis, E.L. (1988) J. Phys. Chem. 92, 6590–6594.
[46] Snare, M J., Treloar, F.E., Ghiggino, K.P. and Thistlewaite, P.J. (1982) J. Photochem. 18, 335–346.
[47] Kramers, H.A. (1940) Physica 7, 284–304.
[48] Lentz, B.R., Barenholz, Y. and Thompson, T.E. (1976) Biochemistry 15, 4521–4528.
[49] Chen, L.A., Dale, R.E., Roth, S. and Brand, L. (1977) J. Biol. Chem. 252, 2163–2169.
[50] Kinoshita, J., Kawato, S. and Ikegami, A. (1977) Biophys. J. 20, 289–305.
[51] Jähnig, F. (1979) Proc. Natl. Acad. Sci. USA 76, 6361–6365.
[52] Quitevis, E.L. and Horng, M.-L. (1990) J. Phys. Chem. 94, 5684–5688.
[53] Houslay, M.D. and Stanley, K.K. (1982) Dynamics of Biological Membranes, pp. 71–81, Wiley, New York.
[54] Worchester, D.L. and Franks, N.P. (1976) J. Mol. Biol. 100, 359–378.
[55] Bush, S.F., Adams, R G. and Levin, I.W. (1980) Biochemistry 19, 4429–4436.